



## Research paper

Probing the geometric structures and electronic properties of anionic and neutral Pt<sub>3</sub>C<sub>2</sub> clusters by density functional calculations

Sheng-Jie Lu

Department of Chemistry and Chemical Engineering, Heze University, Heze, Shandong 274015, China

## ARTICLE INFO

## Article history:

Received 6 January 2018

In final form 24 January 2018

## Keywords:

Geometric structures

Electronic properties

Density functional calculations

## ABSTRACT

We present a theoretical investigation on the geometric structures and electronic properties of Pt<sub>3</sub>C<sub>2</sub><sup>-/0</sup>. The results showed that both anionic and neutral Pt<sub>3</sub>C<sub>2</sub> adopt PtC<sub>2</sub> planar triangular structures with each C atom coordinating with two Pt atoms. Additionally, Pt<sub>3</sub>C<sub>2</sub><sup>-</sup> anion and Pt<sub>3</sub>C<sub>2</sub> neutral both show aromaticity. Bond lengths, bond orders, and constant electronic charge densities of Pt<sub>3</sub>C<sub>2</sub><sup>-/0</sup> suggest that the strong interactions between the two C atoms play vital roles in their structural stability. NPA charge distributions of anionic and neutral Pt<sub>3</sub>C<sub>2</sub> are different. Furthermore, both Pt<sub>3</sub>C<sub>2</sub><sup>-</sup> anion and Pt<sub>3</sub>C<sub>2</sub> neutral have  $\sigma$  plus  $\pi$  double bonding patterns.

© 2018 Elsevier B.V. All rights reserved.

## 1. Introduction

Metal-carbide compounds are very important intermediates in organometallic reactions and have received a great deal of attention due to their extensive application in the catalytic fields [1–3]. Small metal-carbide clusters can be used as useful research models for deeply understanding the important heterogeneous catalytic mechanisms in the organometallic chemistry [4]. Therefore, small M<sub>1–2</sub>C<sub>2</sub> clusters have received considerable attention from both experimental and theoretical points of view. Anion photoelectron spectroscopic studies of MC<sub>2</sub> (M = Sc, V, Cr, Mn, Fe, and Co) suggested that the interactions between the M and C<sub>2</sub> are similar to those between the M and O [5]. Theoretical calculations predicted that the most stable isomer of FeC<sub>2</sub> is cyclic structure [6]. The combined experimental photoelectron spectroscopy and theoretical calculations suggested that only the cyclic isomer of MnC<sub>2</sub><sup>-</sup> contributes to its experimental photoelectron spectrum, whereas both the cyclic and linear isomers of CrC<sub>2</sub><sup>-</sup> contribute to its experimental spectrum [7–9]. Numerous experimental and theoretical investigations were devoted to the encapsulation of M<sub>x</sub>C<sub>2</sub> (x = 2–4, M = Sc, V, Cr, Mn, Fe, and Co) clusters into fullerene carbon cages [10–14]. Anion photoelectron spectroscopy and theoretical studies of Co<sub>n</sub>C<sub>2</sub><sup>-</sup> (n = 1–5) found that their geometric structures can be described as attaching C<sub>2</sub> to the top sites, bridge sites, or hollow sites of Co<sub>n</sub> clusters [15], while the two C atoms were found to be separated gradually with increasing number of V atoms in V<sub>n</sub>C<sub>2</sub><sup>-</sup> (n = 1–6) [16]. The combined experimental and theoretical investigations on Au<sub>1–2</sub>C<sub>2</sub><sup>-/0</sup> revealed that their ground-state structures are linear

configurations and Au atom behaves like H atom in these species [17–19]. However, investigations on multi-metal dicarbon clusters are rather rare, except for some theoretical calculations [20,21]. On the other hand, platinum is one of the most important metal catalysts for mediating C–C bond formation in the cross-coupling reactions [22–26]. Investigations of platinum carbides can provide some insight into the underlying microscopic platinum-catalyzed mechanisms in cross-coupling reactions. In this work, the geometric structures and electronic properties of Pt<sub>3</sub>C<sub>2</sub><sup>-</sup> cluster anion and its corresponding neutral counterpart were investigated by density functional theory (DFT) calculations.

## 2. Theoretical methods

Full structural optimizations and frequency analyses of Pt<sub>3</sub>C<sub>2</sub><sup>-</sup> anion and its neutral counterparts were carried out employing DFT in the context of Beck's three-parameter and Lee–Yang–Parr's gradient-corrected correlation hybrid functional (B3LYP) [27–30]. The augmented correlation-consistent polarized valence triple-zeta (aug-cc-pVTZ) basis set was chosen for C atoms [31], and the aug-cc-pVTZ-PP basis set was used for Pt atoms [32]. No symmetry constraint was imposed during the overall geometry optimizations for both anionic and neutral clusters. The initial structures were obtained by putting the Pt atoms to different adsorption or substitution sites of C<sub>2</sub> framework at all possible spin states. Additionally, the crystal structure analysis by particle swarm optimization (CALYPSO) software was used to search the global minima of Pt<sub>3</sub>C<sub>2</sub><sup>-</sup> anion and its corresponding neutrals [33]. Harmonic vibrational frequency analyses were carried out to confirm that the obtained structures were true local minima on the

E-mail address: [lushengjie@iccas.ac.cn](mailto:lushengjie@iccas.ac.cn)

potential energy surfaces. Zero-point energy (ZPE) corrections obtained from the B3LYP functional were considered in all the calculated energies. Natural population analysis (NPA) was performed to gain insight into the charges distribution of  $\text{Pt}_3\text{C}_2^{-/0}$  using the Natural Bond Orbital (NBO) version 3.1 programs [34–37]. All the calculations and analyses were accomplished using the Gaussian 09 program package [38].

### 3. Theoretical results

The optimized geometries of three low-lying isomers of  $\text{Pt}_3\text{C}_2^-$  and its corresponding neutrals are presented in Fig. 1. In addition, the photoelectron spectrum of the most stable isomer of  $\text{Pt}_3\text{C}_2^-$  is simulated based on the generalized Koopmans' theorem (GKT) [39,40], as displayed in Fig. 2. In the DOS spectrum, the peak of each transition corresponds to the removal of an electron from an individual molecular orbital of  $\text{Pt}_3\text{C}_2^-$ . The first peak associated with the HOMO is set to the position of calculated vertical detachment energy (VDE) of  $\text{Pt}_3\text{C}_2^-$ , and the other peaks associated with the deeper transitions are shifted toward higher binding energies according to their relative energies compared to the HOMO. Then all the calculated peaks are fitted with unit-area Gaussian functions of 0.20 eV full width at half maximum (FWHM).

#### 3.1. $\text{Pt}_3\text{C}_2^-$

The global minimum structure (A) of  $\text{Pt}_3\text{C}_2^-$  anion possesses a  $\text{PtC}_2$  planar triangular framework with the remaining two Pt atoms independently interacting with the two C atoms. Isomer A has  $C_{2v}$  symmetry with an electronic state of  $^2B_1$ . As shown in Fig. 2, the simulated photoelectron spectrum of isomer A suggests that its VDE is small and the peaks at higher EBE region are much congested than those at lower EBE region. The second isomer (B) of  $\text{Pt}_3\text{C}_2^-$  adopts a  $C_s$  symmetric five-membered ring structure with the two C atoms separated by the three Pt atoms and has a  $^2A'$  electronic state. The third isomer (C) of  $\text{Pt}_3\text{C}_2^-$  has a Pt–C–C–Pt chain with the third Pt atom bonding with one of two terminal Pt atoms. Isomers B and C are higher in energy than isomer A by 0.50 and 0.65 eV, respectively.

#### 3.2. $\text{Pt}_3\text{C}_2$

The global minimum (a) of  $\text{Pt}_3\text{C}_2$  neutral has a similar structure with its corresponding anionic counterpart and has a  $^1A_1$  electronic

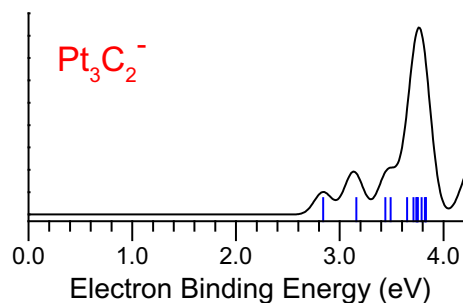


Fig. 2. Simulated photoelectron spectrum of the most stable isomer of  $\text{Pt}_3\text{C}_2^-$  was obtained by fitting the distribution of the transition lines with unit area Gaussian functions of 0.20 eV full widths at half maximum. The vertical lines in blue are the calculated vertical detachment energies for  $\text{Pt}_3\text{C}_2^-$ . (For interpretation of the references to colour in this figure legend, the reader is referred to the web version of this article.)

state. Similar to isomer B, the second isomer (b) of  $\text{Pt}_3\text{C}_2$  adopts a five-membered ring structure with a higher symmetry of  $C_{2v}$ . The third isomer (c) of  $\text{Pt}_3\text{C}_2$  has a  $D_{3h}$  symmetric trigonal bipyramidal structure with the two C atoms located at the apex positions and has an electronic state of  $^1A_1'$ . Isomers b and c are higher than the global minimum (a) in energy by 0.30 and 0.91 eV, respectively.

### 4. Discussion

#### 4.1. Bond lengths, bond angles, and bond orders of $\text{Pt}_3\text{C}_2^{-/0}$

As shown in Fig. 3, the Pt3–C2 and Pt5–C2 bond lengths of  $\text{Pt}_3\text{C}_2^-$  are 1.99 and 1.81 Å, respectively, which are both longer than the Pt–C bond length (1.68 Å) in PtC diatomic molecule,[41] indicating that the interactions between the Pt and C atoms in  $\text{Pt}_3\text{C}_2^-$  are weak than the typical Pt–C double bond in PtC diatomic molecule. This can be further verified by the calculated Wiberg bond orders of Pt3–C2 (0.70) and Pt5–C2 (1.23). The fragmentation energies ( $E_f$ ) of  $\text{Pt}_3\text{C}_2^-$  were calculated as  $E_f(\text{Pt}) = [E(\text{Pt}) + E(\text{Pt}_2\text{C}_2^-) - E(\text{Pt}_3\text{C}_2^-)]$  at the B3LYP level of theory (the  $E$  represents the total energy including zero-point vibrational corrections). The results showed that  $E_f(\text{Pt})$  were calculated to be 350 kJ/mol, which are smaller than the dissociation energies of Pt–C (610 kJ/mol) in PtC diatomic mole-

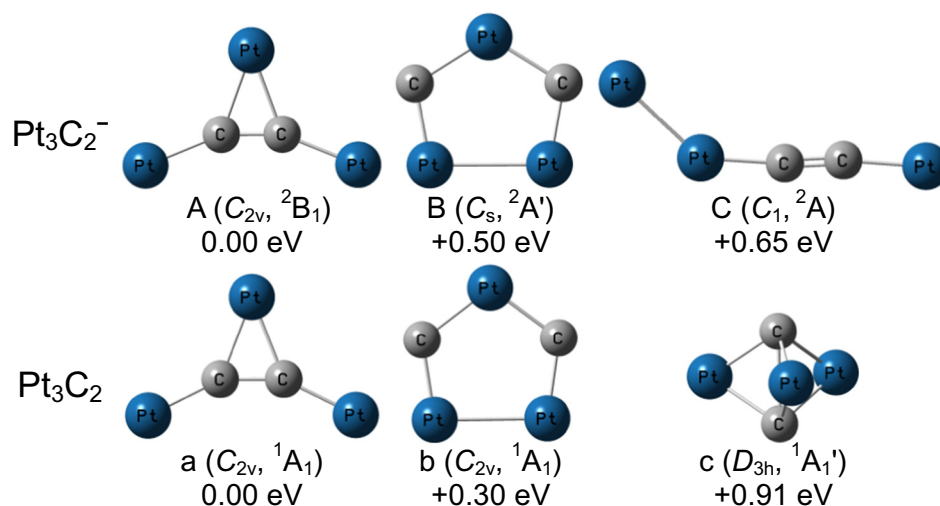


Fig. 1. Typical low-lying isomers of  $\text{Pt}_3\text{C}_2^{-/0}$  obtained at the B3LYP level of theory.

Download English Version:

<https://daneshyari.com/en/article/7838137>

Download Persian Version:

<https://daneshyari.com/article/7838137>

[Daneshyari.com](https://daneshyari.com)